Clinical Cancer Research

Aspirin Inhibits Cancer Metastasis and Angiogenesis via Targeting Heparanase

Xiaoyang Dai[1,2], Juan Yan[1,3], Xuhong Fu[1], Qiuming Pan[1], Danni Sun[1], Yuan Xu[4], Jiang Wang[5], Litong Nie[6], Linjiang Tong[1], Aijun Shen[1], Mingyue Zheng[4], Min Huang[1], Minjia Tan[6], Hong Liu[5], Xun Huang[1], Jian Ding[1], and Meiyu Geng[1]

Abstract

Purpose: Recent epidemiological and clinical studies have suggested the benefit of aspirin for patients with cancer, which inspired increasing efforts to demonstrate the anticancer ability of aspirin and reveal the molecular mechanisms behind. Nevertheless, the anticancer activity and related mechanisms of aspirin remain largely unknown. This study aimed to confirm this observation, and more importantly, to investigate the potential target contributed to the anticancer of aspirin.

Experimental Design: A homogeneous time-resolved fluorescence (HTRF) assay was used to examine the impact of aspirin on heparanase. Streptavidin pull-down, surface plasmon resonance (SPR) assay, and molecular docking were performed to identify heparanase as an aspirin-binding protein. Transwell, rat aortic rings, and chicken chorioallantoic membrane model were used to evaluate the antimetastasis and anti-angiogenesis effects of aspirin, and these phenotypes were tested in a B16F10 metastatic model, MDA-MB-231 metastatic model, and MDA-MB-435 xenograft model.

Results: This study identified heparanase, an oncogenic extracellular matrix enzyme involved in cancer metastasis and angiogenesis, as a potential target of aspirin. We had discovered that aspirin directly binds to Glu225 region of heparanase and inhibits the enzymatic activity. Aspirin impeded tumor metastasis, angiogenesis, and growth in heparanase-dependent manner.

Conclusions: In summary, this study has illustrated heparanase as a target of aspirin for the first time. It provides insights for a better understanding of the mechanisms of aspirin in anticancer effects, and offers a direction for the development of small-molecule inhibitors of heparanase. *Clin Cancer Res; 23(20); 6267–78.* ©*2017 AACR.*

Introduction

Aspirin, a classical NSAID, has been used in broad conditions including fever, pain, and inflammatory disease (1). Recently, many epidemiological, clinical, and experimental studies have shown that long-term use of aspirin can significantly reduce the incidence of cancer, delay the malignant process, impair the risk of tumor metastasis, and decrease cancer mortality (2–9). Although the benefit of aspirin for patients with cancer has been widely appreciated, the mechanism behind remains largely unclear. Previous understandings tend to attribute the anticancer potential of aspirin to the inhibition of cyclooxygenase-2 (COX-2), which is upregulated in various cancer cells (10, 11). Of note, increasing evidence has suggested that aspirin may exhibit anticancer effects in a COX-independent manner. An apparent discrepancy is that the concentrations required to exert these effects in cancer cells were significantly higher than that required to inhibit the activity of COX-1 or COX-2, suggesting the implications of other potential targets (12, 13). Indeed, cell-based studies have demonstrated that aspirin inhibits cell proliferation, induces cell-cycle arrest and apoptosis in multiple cancer cell lines irrespective of COX-2 expression level (14–18). Aspirin can also sensitize cancer cell to TRAIL-induced apoptosis through a COX-2-independent mechanism (19). Clinical studies confirmed that the benefit of aspirin appears unrelated with COX-2 inhibition but with other proteins, such as PIK3CA and HLA class I antigen (20–22). As such, it is of importance to characterize the target spectrum of aspirin in cancer cells and demonstrate their association with the anticancer potential of aspirin. Hence, we employed proteomic study by using biotin–aspirin to identify aspirin associated proteins, and discovered heparanase as one of the potential targets of aspirin in cancer cells.

Heparanase is an endo-β-D-glucuronidase that degrades the heparan sulfate (HS) chain of heparan sulfate proteoglycans (HSPG) on the tumor cell surface and in the extracellular matrix (ECM; refs. 3, 24). As the only HS degrading endoglycosidase

[1]Division of Anti-Tumor Pharmacology, State Key Laboratory of Drug Research, Shanghai Institute of Materia Medica, Chinese Academy of Sciences, Shanghai, P.R. China. [2]Zhejiang Province Key Laboratory of Anti-Cancer Drug Research, College of Pharmaceutical Sciences, Zhejiang University, Hangzhou, P.R. China. [3]University of Chinese Academy of Sciences, Beijing, P.R. China. [4]Drug Discovery and Design Center, State Key Laboratory of Drug Research, Shanghai Institute of Materia Medica, Chinese Academy of Sciences, Shanghai, P.R. China. [5]Key Laboratory of Receptor Research, Shanghai Institute of Materia Medica, Chinese Academy of Sciences, Shanghai, P.R. China. [6]The Chemical Proteomics Center, Shanghai Institute of Materia Medica, Chinese Academy of Sciences, Shanghai, P.R. China.

Note: Supplementary data for this article are available at Clinical Cancer Research Online (http://clincancerres.aacrjournals.org/).

X. Dai and J. Yan contributed equally to this article.

Corresponding Authors: Meiyu Geng, Shanghai Institute of Materia Medica, Chinese Academy of Sciences, 555 Zuchongzhi Road, Shanghai 201203, P.R. China. Phone: 86-21-50806600-2409; Fax: 86-21-50806072; E-mail: mygeng@simm.ac.cn; Xun Huang, xhuang@simm.ac.cn; and Jian Ding, jding@simm.ac.cn

doi: 10.1158/1078-0432.CCR-17-0242

Translational Relevance

The anticancer potential of aspirin, a classical nonsteroidal anti-inflammatory drug, has been widely recognized and intrigued broad interest to explore the clinical benefits of aspirin in cancer therapy. However, the current understanding of molecular mechanisms of aspirin remains very limited. This study identified heparanase, an enzyme degrading polymeric heparan sulfate at the cell surface and within the extracellular matrix, as a potential target of aspirin. The study provides experimental evidence showing that aspirin impeded tumor metastasis and angiogenesis, by inhibiting the enzymatic activity of heparanase. These findings gain mechanistic insights into the anticancer activity of aspirin and may provide useful information for the clinical explorations of aspirin in cancer treatment. This study also offers a new direction for the development of small-molecule inhibitors of heparanase.

involving in ECM degradation, heparanase critically remodels tumor microenvironment to facilitate tumor cell migration and invasion in cancer metastasis (25–27). Heparanase caused ECM collapse also led to release of heparin-binding cytokines like HGF, VEGF, and bFGF which promote tumor angiogenesis (26, 27). Such an irreplaceable role in cancer metastasis and angiogenesis makes heparanase an appealing target for cancer therapy (28–33). However, there is no heparanase inhibitor available in clinical to date.

This study aims to explore the interaction between aspirin and heparanase, and to demonstrate biological significance to complement aspirin's pharmacological effects.

Materials and Methods

Cell culture

Human cancer cell line MDA-MB-435 and MDA-MB-231 were purchased from ATCC; U87-MG was obtained from the Institute of Biochemistry and Cell Biology (Chinese Academy of Sciences); primary human umbilical vascular endothelial cells (HUVECs) were purchased from AllCells. CHO-K1 and B16F10 were purchased from Japanese Collection of Research Bioresources (JCRB, Japan). All the cell lines used in this study were obtained during 2000 to 2012 and cultured according to the suppliers' instructions. Cells were checked to confirmed to be mycoplasma-free, and the cells were passaged no more than 25 to 30 times after thawing. Cell lines were characterized by Genesky Biopharma Technology using short tandem repeat (STR) markers (latest tested in 2017).

Homology modeling of human heparanase

The FASTA sequence of human heparanase was retrieved from NCBI protein sequence database (Accession: Q9Y251). Four steps were followed to develop the homology model of human heparanase. (i) Templates selection. The BLAST program was used to search suitable template available in the PDB (34). The crystal structure of beta-glucuronidase (PDB:3VNZ) from Acidobacterium Capsulatum with a resolution of 1.8 Å was obtained, shared 24% sequence identity with human heparanase (35). (ii) Sequence alignment. Sequences of human heparanase (Q9Y251) and β-glucuronidase were aligned in MODELLER 9.13 (36). (iii) Model Generation. Five individual models were generated with MODELLER 9.13, and the one with the highest DOPE score was chosen for further study. (iv) Model Validation. The model was validated by PROCHECK analysis.

Molecular docking

The three molecules, aspirin, biotin–aspirin, and salicylic acid, were prepared using the LigPrep module (LigPrep, version 2.4; Schrödinger, LLC) to generate low-energy three-dimension conformation. The homology model of human heparanase was prepared using Protein preparation wizard tool in the Maestro (Maestro, version 9.0; Schrödinger, LLC), including verifying proper assignment of bonds, adding hydrogens, deleting unwanted bound water molecules and minimizing protein energy with the OPLS2005 force field. All the parameters in this module were used with default values unless noted. Then ligands were docked with Induced Fit Docking (IFD) protocol in Maestro (Maestro, version 9.0; Schrödinger, LLC). The binding site of the ligand in 3VNZ was used as the reference to define the active site of human heparanase. A 14 Å × 14 Å × 14 Å grid box encompassing the predefined active sites was established. In IFD, Prime (Prime, version 2.2; Schrödinger, LLC) was used to refine residues within 5.0 Å of ligand poses. All the parameters in this process were used with default values unless noted. Finally, top-ranked 50 binding poses (in terms of IFDScore) of each ligand were remained for further analysis.

Construction of stably heparanase-expressing cell lines

Cells were transfected with the heparanase expression vector, pBABE/myc-His-C-hpse-kozak (constructed by our lab), using Lipofectamine 2000 (Life Technologies, Inc.). Transfected cells were selected with 1 μg/mL puromycin in culture medium for 1 week. Then cells were analyzed for exogenous heparanase expression, using Western blotting with a heparanase antibody.

RNA interference and clone construction

Cells were seeded on six-well plates, and the medium was replaced with Opti-MEM I Reduced Serum Media (Invitrogen) containing 50.0 nmol/L siRNA (GenePharma, China) and Lipofectamine RNAiMAX transfection reagent (Invitrogen) according to manufacturer's recommendations. The sense sequence of the COX-1 siRNA-5#, COX-2 siRNA-6#, and COX-2 siRNA-7# were 5′-GUGAAUCCCUGUUGUUACUTT-3′, 5′-GCUCCGGACUAGAUGAUAUTT-3′, and 5′-GCUUUAUGCUGAAGCCCUATT-3′, respectively. The PLATINUM Select Human MLP Retroviral shRNA-mir-Target heparanase plasmid and empty vector (Transomic) were transfected into cells using the X-tremeGENE HP DNA Transfection Reagent (Roche) as recommended by the manufacturer.

Homogeneous time-resolved fluorescence-based heparanase activity assay

Human recombinant heparanase was expressed in insect cells and purified as our previous report (37). Briefly, 1.0 μL compound and 4.0 μL of heparanase solution or 5.0 μL heparanase dilution buffer were added into 384-well plate. After 10 minutes preincubation at 37°C, an enzyme reaction was initiated by adding 5.0 μL of Bio-HS-Eu(K) (Cisbio International) and the 384-well plate was incubated for 150 minutes at 37°C. To stop the enzyme reaction and detect the remaining substrate, either 10 μL of a 1.0 μg/mL XL665-labeled streptavidin (Cisbio International)

solution or dilution buffer was added into plate. After a 30-minute incubation at RT, the HTRF signal was measured using an Envision plate reader (Perkin Elmer) using the following setup: excitation 337 nm, emissions 620 nm and 665 nm.

Pull-down and MS analysis of aspirin-bound proteins

MDA-MB-435 and U87-MG-HPA cell were cultured in 10 cm dish. And the cell lysates were incubated with biotin or biotin-aspirin in the absence or presence of unlabeled aspirin for 4 hours at 4°C, then addition of prewashed Streptavidin beads (GE Health), incubated overnight at 4°C. The bead-bound proteins were separated by SDS-PAGE and analyzed with a monoclonal antihuman heparanase1 antibody (Antibody Clone HP130, InSight Biopharmaceuticals Ltd.), or visualized by sliver staining, followed by in-gel digestion and finally analyzed by nano LC/MS-MS.

Nano LC/MS-MS analysis of biotin–aspirin-binding proteins

Tryptic peptides from each band were dissolved in solvent A (0.1% formic acid, 2% acetonitrile, 98% H_2O). Samples were then injected onto a manually packed reversed phase C18 column (170-mm × 79-μm, 3-μm particle size; Dikma) coupled to Easy nLC 1000 (Thermo Fisher Scientific). Peptides were eluted from 7% to 40% solvent B (0.1% formic acid in 90% acetonitrile and 10% H_2O) in solvent A (0.1% formic acid in 2% acetonitrile and 98% H_2O) with a 60-minute gradient, and 40% to 80% with 10-minute gradient at a flow rate of 300 nL/min. The fractions were analyzed by using a Q-Exactive mass spectrometer. For full MS spectra, the scan range was 350 to 1300 with a resolution of 70,000 at m/z 200. For MS/MS scan, the 16 most intense ions above 2×10^4 with charge state two to six in each full MS spectrum were sequentially fragmented by high-collision dissociation (HCD) with normalized collision energy 28%, then ion fragments were detected in the Orbitrap at a resolution of 17,500 at m/z 200. The dynamic exclusion duration was set as 30 seconds, and the isolation window was 2 m/z. Automatic gain control (AGC) was used to prevent overfilling of the ion trap.

MS database search

All MS raw files were analyzed by Mascot software (version2.3.01) against the database Uniprot_Human_histone (updated in 20150929) to identify the proteins. Acetylation (Protein N-term) and oxidation (M) were specified as variable modifications. Other parameters were as follows: mass error for parent ion mass was ±10 ppm with fragment ion as ±0.02 Da and enzyme was trypsin with three maximum missing cleavages. Peptide ion score cutoff was 20, and protein score cutoff was 30. When a protein was matched by only one or two peptides, the spectrum was manually checked (38).

Western blotting

Cell lysates were determined with the BCA method, and an equal amount of proteins was separated by SDS–PAGE and then transferred to nitrocellulose membranes. The membranes were blocked with 5% (w/v) non-fat dry milk, followed with overnight incubation at 4°C with the following antibodies: monoclonal antihuman heparanase1 (Antibody Clone HP130, InSight Biopharmaceuticals Ltd.; 1:1000), anti-Src (#2108S; 1:1,000), anti-phospho-Src (Tyr 416, #2101S; 1:1,000), anti-Erk1/2 (#9102S; 1:1,000), anti-phospho-ERK1/2 (Thr202/Tyr204, #9101; 1:1,000) anti-p38 (#9212), anti-phospho-p38 (Thr180/Tyr182, #9211; 1:1,000), anti-Akt (#9272; 1:1,000), anti-phospho-Akt (Ser473, #4060; 1:1,000), anti-Stat3 (#4904; 1:1,000), anti-phospho-Stat3 (Tyr705, #9145; 1:1,000), anti-Stat5 (#9352; 1:1,000), anti-phospho-Stat5 (Tyr694, #9351; 1:1,000; all antibodies except Monoclonal antihuman heparanase were purchased from Cell Signaling Technology, Inc.), anti-JAK2 (ab68269, Abcam; 1:500), anti-phospho-JAK2 (Y1007/1008, ab68268, Abcam; 1:500), anti-GAPDH antibody (KangChen Bio-tech). Immunoreactive proteins were detected using ECL Plus (Thermo Fisher Scientific), after secondary antibody incubation (Jackson Immuno Research Laboratories Inc.).

Cell migration and invasion

Transwell chambers (8 μm pore size; Corning Life Sciences) were coated with 100 μL of diluted Matrigel or not. 0.6 mL medium containing 10% FBS was added to the lower chambers, and cells suspended in serum-free medium at a density of 1.5×10^5 cells/mL (doubled for invasion) were seeded (0.1 ml) in the upper chambers. Various concentrations of aspirin were added to both of the upper and lower chambers. After cultured for appropriate time (i.e., 24 hours for MDA-MB-435), cells were then fixed by cold 95% ethanol, stained by 0.1% crystal violet, and cells that had not migrated were removed from the upper chambers. The remaining cells were photographed. The dye was dissolved in 80 μL of 10% acetic acid, and the absorbance of the resulting solution was measured at 600 nm using a multiwell spectrophotometer (SpetraMAX190; Molecular Devices).

Assaying the release of VEGF

Cells, suspended in medium containing 10% FBS, were plated at the same density in six-well plates. After adherence, replaced the medium with serum-free medium, and various concentrations of aspirin were added. After 24 hours, conditional media were collected and the quantity of VEGF was analyzed using Elisa Kit (Maibio, CHN).

Tube formation assay

Ninety-six-well plates were precoated with 60 μL liquid Matrigel per well. After incubated at 37°C for 1 hour, HUVECs (1.5×10^4 cells/well), suspended in M199 medium with different concentrations of aspirin, were seeded and further cultured for 8 hours. Tubes were imaged by an inverted phase contrast microscope (IX70, Olympus) and the enclosed networks of complete tubes from five randomly chosen fields were photographed and counted.

Rat aortic ring assay

This animal study was conducted in accordance with the rules and regulations of the Institutional Animal Care and Use Committee (IACUC) at Shanghai Institute of Materia Medica. The aortas were obtained from Sprague–Dawley rats. Six-week-old SD rats, were obtained from the Shanghai Institute of Materia Medica. Each aorta was cut into 1-mm slices and embedded in 60 μL Matrigel in 96-well plates. The aortic rings were then cultured in 100 μL of M199 medium with 20% FBS, 30 μg/mL ECGS, 10 ng/mL EGF, and various concentrations of aspirin, and photographed on day 7.

Chick chorioallantoic membrane assay

Fertilized chicken eggs were pre-incubated to grow for 7 days. Gentle suction was applied to the hole located at the broad end of

the egg to create a false air sac directly over the chick chorioallantoic membrane (CAM), and a 1 cm^2 window was immediately removed from the eggshell. Slides (0.5 cm × 0.5 cm) were pretreatment with aspirin (1, 2, and 4 mmol/L) or suramin (1 and 10 μmol/L) by dropping 1 mL solution on one slide. At the next day, the slides were dried up and placed on areas between preexisting vessels, and the embryos were further incubated for 48 hours (39). The neighboring neo-vascular zones were photographed with a stereomicroscope (MS5; Leica).

Murine B16F10 and human breast cancer MDA-MB-231 experimental lung metastasis assay

This animal study was conducted in accordance with the rules and regulations of the IACUC at the Department Of Laboratory Animal Science, Fudan University (Shanghai, P.R. China) and Zhejiang University (Hangzhou, P.R. China). B16F10 and MDA-MB-231 cells were collected and resuspended in serum-free medium. C57/BL6 mice (Balb/c nu mice for MDA-MB-231) were injected through the tail vein with 5×10^5 cells in 0.2 mL, and after that, mice were immediately treated with a different dosage of aspirin or 0.5% CMC-Na. One week later (B16F10 metastasis model, 3 weeks later for MDA-MB-231 metastasis model), animals were sacrificed, and lungs were fixed in 4% paraformaldehyde or Bouin's solution and counted the number of metastatic nodules on the lung surface.

Subcutaneous xenograft model in athymic mice

This animal study was conducted in accordance with the rules and regulations of the IACUC at the Department Of Laboratory Animal Science, Fudan University. Female Balb/c nude mice, 4 to 5 weeks old, were purchased from Shanghai Slac Laboratory Animal Limited Company. Tumor cells at a density of 5×10^6 in 0.2 mL PBS were injected subcutaneously into the right flank of nude mice. When tumors reach around 100 mm^3 at about 2 weeks, the mice were randomly assigned to three groups, control (0.5% CMC-Na), aspirin 125 and 250 mg/kg. Tumors and body weight of mice were measured individually triple per week. After treatment for 3 weeks, mice were sacrificed after the final therapy. The tumors were removed, some were fixed 4% paraformaldehyde and stained with anti-CD31 antibody (ab28364; Abcam), and the other tumors were lysed for Western blotting.

Statistical analysis

Student *t* tests were performed as indicated in the figures. Results were considered significant when $P < 0.05$ (*, $P < 0.05$; **, $P < 0.01$; and ***, $P < 0.001$).

Results

Aspirin directly binds to heparanase and inhibits its activity

In a previous effort to identify the potential targets of aspirin in cancer cells, we conducted a proteomic study using biotin-tagged aspirin as a chemical probe to pull-down aspirin-associated proteins (Fig. 1A, a), and discovered heparanase as a potential aspirin-associated protein detected by mass spectrometry (Supplementary Table S1 and Supplementary Fig. S1A). We confirmed this observation by incubating biotin–aspirin with cell lysates of MDA-MB-435 and U87-HPA cells stably transfected with heparanase. The free biotin was used as a negative control. Streptavidin-pull down followed by SDS-PAGE gel electrophoresis analysis discovered that heparanase was pulled down by biotin–aspirin, but not by biotin. And the aspirin binding of heparanase was competed by higher concentrations of unlabeled aspirin (Fig. 1A, b), suggesting the specific binding of aspirin to heparanase.

Aspirin inhibits heparanase enzymatic activity in cancer cells

We next explored the biological significance of the heparanase binding. To this end, a HTRF-based biochemical assay was used to measure the impact of aspirin on the heparanase activity. Suramin, known as an inhibitor of heparanase, was used to validate the assay (Supplementary Fig. S2A). We found that aspirin inhibited heparanase activity with an IC_{50} of 3.55 mmol/L (Fig. 1B). We also examined the activity of salicylic acid, the main hydrolysis products of aspirin in cells. Salicylic acid similarly showed inhibitory effect on heparanase activity (Supplementary Fig. S2B), suggesting the potential of aspirin in inhibiting cellular heparanase activity. After treatment with different concentrations of aspirin, the heparanase activity were detected by HTRF assay with the same amount of protein in B16F10 (8 hours), CHO-K1 (12 hours), MDA-MB-435, and U87-MG (24 hours). Indeed, incubation of aspirin with these cancer cells led to a dose-dependent inhibition of cellular heparanase activity (Fig. 1C).

Aspirin directly binds to Glu225 region of heparanase to inhibit enzymatic activity

The results above provided the first evidence demonstrating aspirin as an enzymatic inhibitor of heparanase. We were interested in understanding how aspirin inhibits heparanase activity. Substrate competition is reported as a common mechanism of small molecule inhibitors, such as PI-88, to inhibit heparanase activity. Hence, we tested whether aspirin directly binding to heparin-binding domains of heparanase using a surface plasmon resonance assay. Three domains (KKDC, QPLK, KKLR) known to mediate heparin and heparan sulfate binding to heparanase were tested. But we did not observe the binding of aspirin to either of these domains (Fig. 2A–C), indicating that aspirin may bind to non-heparin binding sites.

The binding site of aspirin was explored using molecular docking with the homology model of human heparanase. Most of the top-ranked conformations of aspirin showed the same binding mode in human heparanase (Fig. 3A). The oxygen in carboxyl group interacted with Glu225, Ser228, and Lys231, whereas acetyl group formed hydrogen bonds with Gln157 and Lys159. The hydrogen bonds formed between the carboxyl group and Glu225 and Lys231 were also reported in Sapay's work (40). We further investigated the binding modes of biotin–aspirin and heparanase (Fig. 3B). The oxygen atom of acetyl group also bound to the Lys159, and the aldehyde group (the original carboxyl group of the aspirin connected with biotin) interacted with Ser228 and Lys231. The aspirin fragment of Biotin-aspirin also located in this pocket with the same interaction pattern.

The binding modes of aspirin and salicylic acid (degradation product of aspirin) were compared (Fig. 3C). Strikingly, the result showed that majority top-ranked conformations of salicylic acid are completely consistent with aspirin. The carboxyl group and phenolic hydroxyl of salicylic acid formed hydrogen bonds with Glu225, Ser228, Lys231, and Gln157. All of these showed that aspirin, salicylic acid and biotin–aspirin should bind to heparanase in the same way (Fig. 3D), and highlighted the important role of Glu225, Lys231, Gln157, and Lys159 in these interactions.

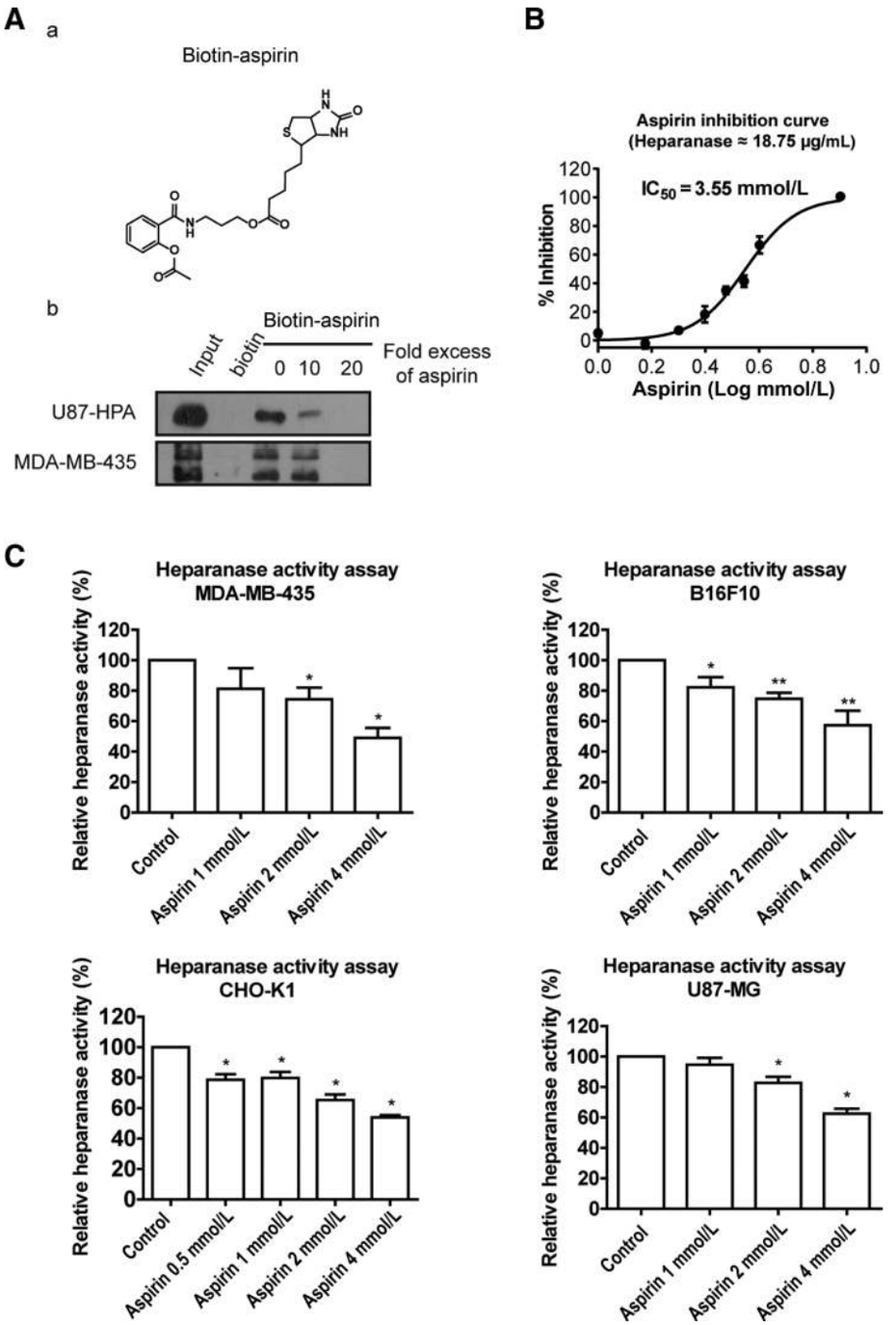

Figure 1.
Aspirin inhibits heparanase activity through directly binding to it. **A,** Structure of biotin–aspirin (a). MDA-MB-435 and U87-HPA (heparanase overexpression) cell lysates were incubated with biotin–aspirin or biotin in the absence or presence of a 10- or 20-fold excess of unlabeled aspirin, followed by pull-down with streptavidin-agarose. The precipitates were detected by Western blotting for heparanase proteins (b). **B,** The inhibition curve of aspirin to heparanase which was purified from *T.ni* cell. The heparanase activity was assayed by HTRF. **C,** The effect of aspirin on heparanase activity inhibition in different cells. Various concentrations of aspirin were added to MDA-MB-435, B16F10, CHO-K1, and U87-MG cell. After cell lysates were quantified by BCA assay, taking the equal amounts of proteins to determine the heparanase activity by HTRF assay. Data are shown as means ± SE of three independent experiments. *, $P < 0.05$.

To verify this possibility, we used point mutations to classify which point or points is/are important for aspirin binding to heparanase. The result of Western blot analysis showed that the biotin–binding activity was decreased when Glu225, Lys231, Gln157, and Lys159 single-point mutation, especially, Glu225 and Lys159 point mutation. Furthermore, double point mutations Gln157/Lys159, Gln157/Lys231, and Glu225/Lys159 proved the key binding sites might be Glu225 and Lys159 (Fig. 3E). Meanwhile, we examined whether these point mutations have any effect on the heparanase activity. It was shown that Glu225 mutation caused inactivation of heparanase, whether Lys159 was not a key site for heparanase activity (Fig. 3F). All of the results above demonstrated aspirin directly binds to Glu225 region of heparanase.

Aspirin inhibits heparanase-promoted cell migration and invasion

As heparanase has been correlated with the metastatic potential of tumor cells, we used a transwell chamber to test the effects of aspirin on heparanase-associated migration and invasion.

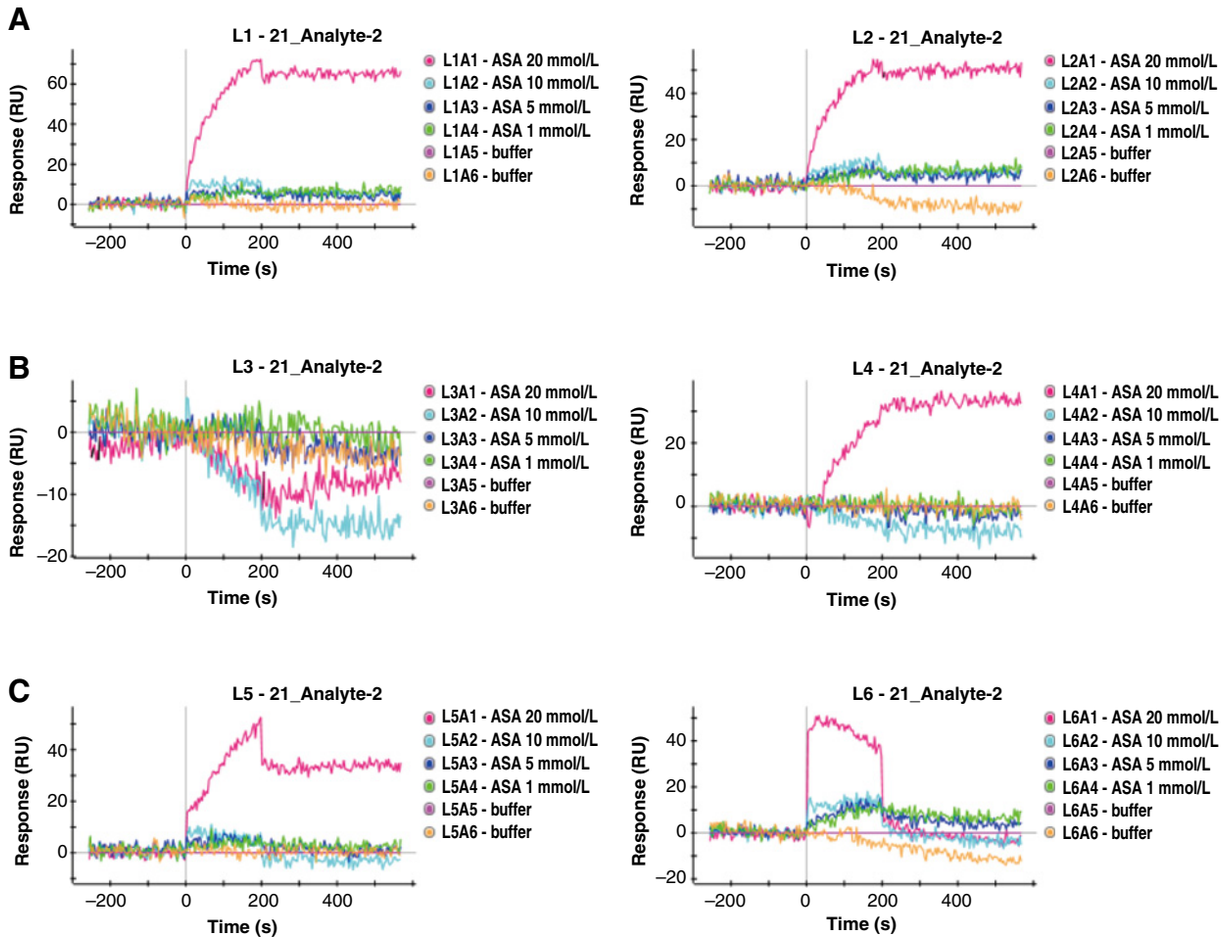

Figure 2.

Surface plasmon resonance analysis. Binding response curves of interactions between aspirin with peptides KKDC (**A**), QPLK (**B**), KKLR (**C**), and scramble controls immobilized on the sensor chip. Concentrations of aspirin are 1, 5, 10, and 20 mmol/L from bottom to top. Representative of three independent experiments with similar results.

B16F10 and MDA-MB-435, which have high-level expression of heparanase, were treated with aspirin. Results showed that aspirin dose-dependently decreased the proportion of migrated cells, with 1 mmol/L aspirin yielding 69.3% inhibition rate in B16F10 cells (Fig. 4A), 4 mmol/L aspirin yielding 63.4% inhibition rate in MDA-MB-435 cells (Fig. 4B).

To test whether the aspirin abrogated cell migration via inhibiting heparanase, we examined the impact on migration and invasion of CHO cells stably expressing heparanase (CHO-HPA). Heparanase overexpression decreased the inhibitory rate of aspirin from 49.5% to 3.1% in cell migration assay (at 2 mmol/L) and from 32.7% to 18.8% in cell invasion assay (at 4 mmol/L; Fig. 4C). When depleting heparanase in MDA-MB-435 cells, the effect of aspirin was abolished on migration and invasion (Fig. 4D). Similar effect was also verified in MDA-MB-231 cell (Supplementary Fig. S3E). Likewise, exogenous addition of heparanase rescued the impaired invasion of MDA-MB-231 cells caused by aspirin treatment (data not shown). In consideration of that aspirin has COX-dependent antitumor activity, we used siRNA to knockdown COX and dissected aspirin's effect. Obviously, aspirin was able to inhibit MDA-MB-231 breast cancer cell migration and invasion regardless of COX-1 or COX-2 depletion, suggesting a COX-independent manner (Supplementary Fig. S3A and S3B). All these results collectively suggested a heparanase-dependent effect of aspirin in inhibiting cancer cell migration and invasion.

Aspirin combats heparanase-promoted VEGF release and tumor angiogenesis

Heparanase is known to promote the release VEGF and other heparan sulfate-bound angiogenic growth factors accelerating pro-angiogenic factors-driven angiogenesis. Hence, we examined the effects of aspirin on VEGF release from tumor cells. The level of VEGF secreted into the culture medium of cancer cells was measured by ELISA. The results showed that treatment with aspirin significantly inhibited VEGF release in MDA-MB-435 and U87-MG cells (Fig. 5A, top), whereas heparanase overexpression in CHO or silencing in MDA-MB-435 reversed the effect of aspirin on promoting VEGF release (Fig. 5A, bottom).

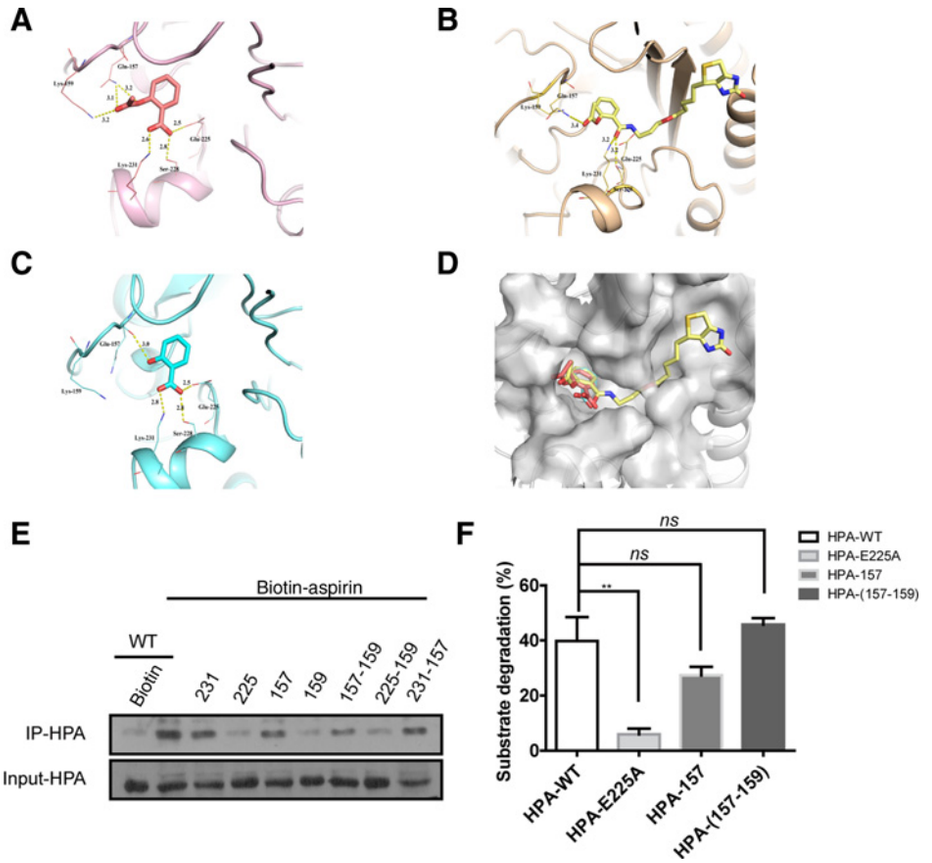

Figure 3.
Comparison between the binding modes of aspirin, biotin–aspirin, and salicylic acid. The binding mode of aspirin (**A**), biotin-aspirin (**B**), and salicylic acid (**C**) in human heparanase. Compounds are shown in sticks and important residues are shown in lines. **D,** The alignments of all three compounds in human heparanase. **E,** The Streptavidin-pull down assay was immunoblotting with anti-heparanase antibody after biotin-aspirin incubated with phoenix-293 transfected with heparanase or point mutations. **F,** The enzyme activity of different types of heparanase were assayed by HTRF.

The released VEGF and other pro-angiogenic factors from tumor cells are able to promote tumor angiogenesis via stimulating vascular endothelial cells. Hence, we also measured the impact of aspirin on tumor angiogenesis using a tube formation assay. Tube formation of human umbilical vein endothelial cells (HUVEC) was shown as formation of complete network structures on Matrigel within 8 hours serum stimulation. After aspirin treatment, the tubule formation was suppressed in a dose-dependent manner. Two mmol/L aspirin resulted in an inhibition rate of approximately 32.9%, and we observed nearly complete suppression at the concentration of 4 mmol/L (Fig. 5B). Similarly, aspirin can inhibit the tube formation, even at the presence of celecoxib or rofecoxib. Celecoxib and rofecoxib had no detectable effect on angiogenesis even at 5 μmol/L, higher than the selective dose for the COX-2 enzyme activity. Suramin, a heparanase inhibitor, can inhibit tube formation. Although suramin and aspirin were added simultaneously, there was still no detectable effect on angiogenesis (Supplementary Fig. S4A). These results supported the conclusion that aspirin inhibited tube formation through a heparanase-dependent instead of a Cox-independent manner. We further confirmed the anti-angiogenic effects of aspirin using aorta sprout outgrowth assay, an *ex vivo* method that recapitulates the key steps in the angiogenesis process. As shown in Fig. 5C, aspirin at 4 mmol/L completely inhibited the outgrowth of new microvessels. Moreover, we also examined the effects of aspirin on the new blood vessel formation process using the CAM assay. Similarly, neovascularization in chick embryos was significantly inhibited when they were treated with aspirin (1, 2, or 4 mmol/L per egg), compared with the nontreated control (Fig. 5D). All these results demonstrated that aspirin possessed an anti-angiogenic potential *in vitro* and *ex vivo*.

Aspirin inhibits cancer antimetastatic and anti-angiogenic activity *in vivo*

Our aforementioned results have suggested heparanase-dependent antimetastatic and anti-angiogenic activity of aspirin *in vitro*. We further confirmed the effects *in vivo*. The antimetastatic potential of aspirin was assessed using a murine B16F10 experimental metastasis model, shown to exhibit heparanase secretion associated metastatic potential (28). Daily treatment of aspirin at dosages of 62.5, 125, and 250 mg/kg was started on the same day following B16F10 injection and the treatment lasted for 1 week. At the termination of the study, the total number of melanoma colonies (dark spots) on the lung surface was counted. Significant metastases were observed in the control group treated with vehicle, which was dramatically decreased following aspirin treatment (Fig. 6A, left), yielding inhibition rates of 19.9%, 49.6%, and 65.5%, at 62.5, 125, and 250 mg/kg, respectively (Fig. 6A, right). Furthermore, we verified the inhibition of aspirin in MDA-MB-231 lung metastasis model. Aspirin could suppress metastasis incidence rate *in vivo*. Especially, 200 mg/kg of aspirin decreased the metastases number, $P < 0.05$ (Supplementary Fig. S3D). These results confirmed the antimetastatic activity of aspirin *in vivo*.

We also examined the anti-angiogenic activity of aspirin in a heparanase-associated xenograft model by subcutaneously injecting human breast cancer MDA-MB-435 cells in nude mice. Following a 20-day administration, tumor growth inhibition was

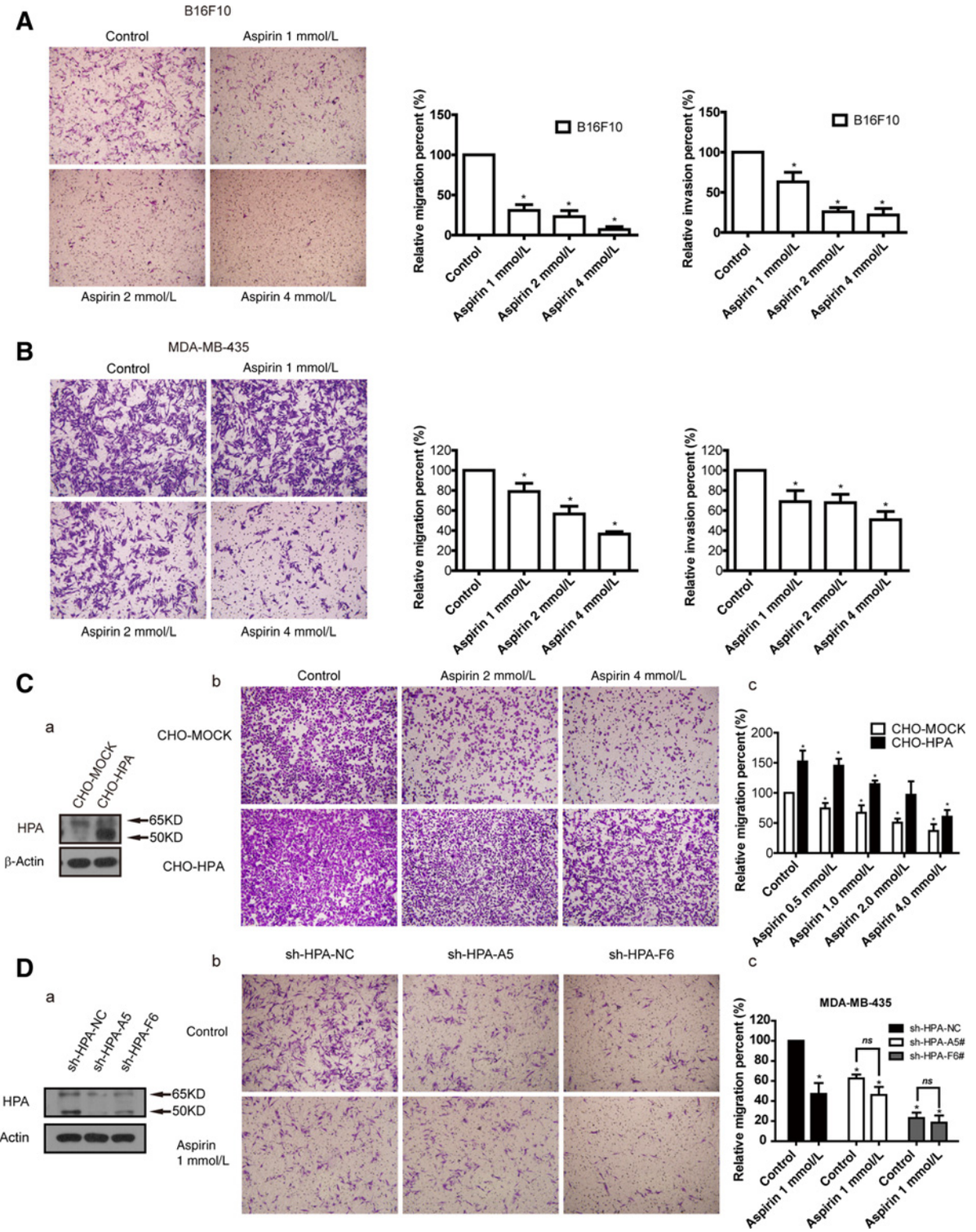

Figure 4.

The inhibitory effect of aspirin on the migration and invasion of different cells. The inhibitory effect of aspirin on migration and invasion of serum-stimulated murine myeloma B16F10 (**A**) and human breast tumor MDA-MB-435 cells (**B**) *in vitro*. The migration and invasion capacity were assessed after 8 hours (B16F10) or 24 hours (MDA-MB-435) as described in the Materials and Methods. The inhibitory effect of aspirin on migration and invasion of serum-stimulated stably heparanase overexpression CHO-HPA (**C**) and knockdown of heparanase in MDA-MB-435 (**D**) cell *in vitro*. a, Western-blotting analysis of heparanase expression. b, After 8 hours (CHO-MOCK/HPA cell) or 24 hours (MDA-MB-435/SH-HPA cell) treatment of aspirin, the migration and invasion capacity were detected. c, quantification of the inhibition activity of aspirin on migration. Data are shown as means ± SE of three independent experiments. *, $P < 0.05$; ns, nonsignificant.

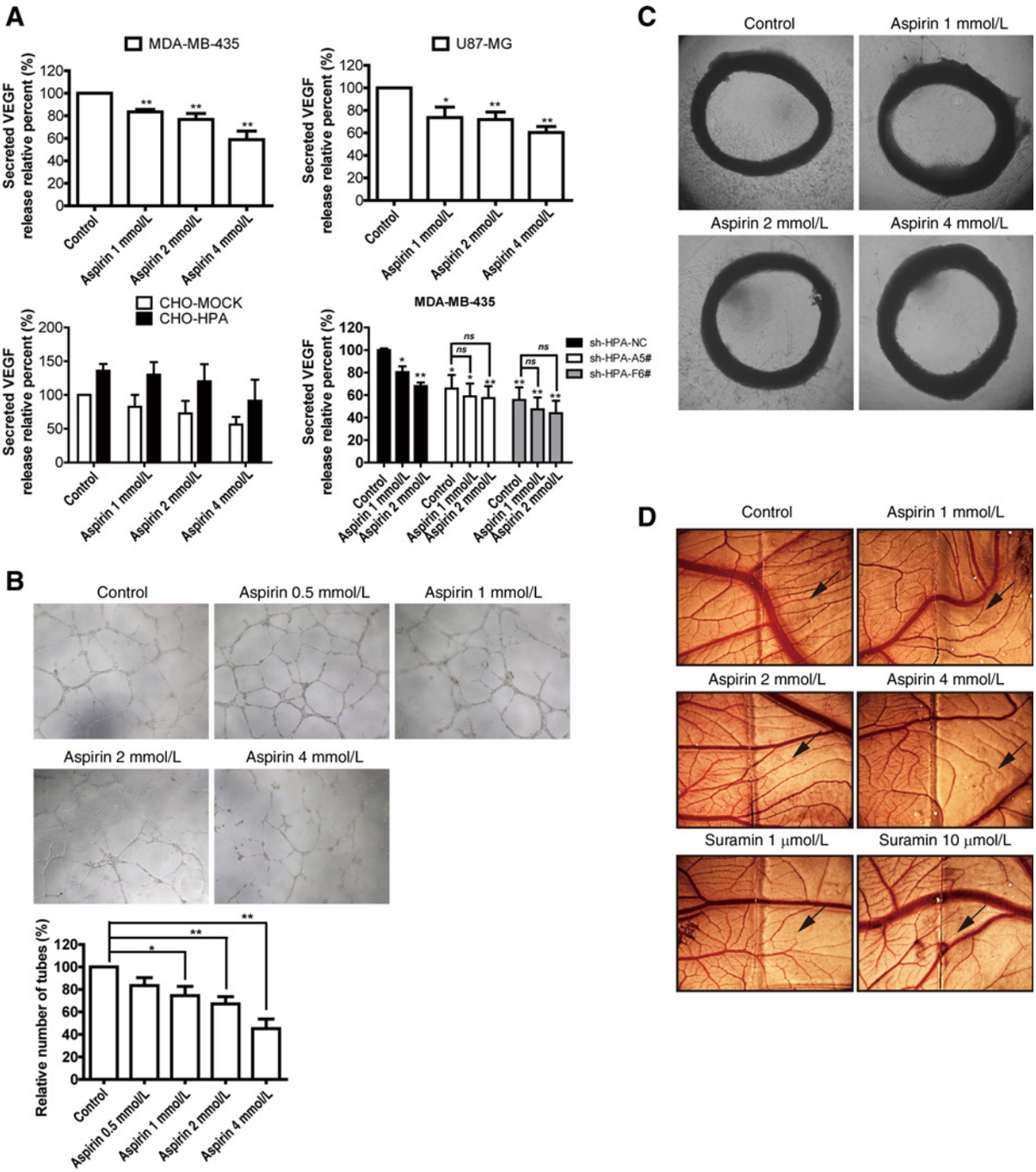

Figure 5.

Aspirin inhibits the VEGF release and suppresses angiogenesis. **A,** Aspirin concentration-dependently inhibits VEGF secretion. MDA-MB-435, U87-MG, and CHO cells were cultured in FBS-free medium and treated with indicated concentrations of aspirin for 12 hours (CHO cells) or 24 hours (MDA-MB-435 and U87-MG cells). VEGF levels were detected with ELISA Kit. Columns, mean of triple replicates; bars, SEM. **B,** Effect of aspirin against HUVEC tube formation on Matrigel. HUVECs seeded on Matrigel in medium were treated with aspirin for 8 hours. Top, representative photographs of three independent experiments were shown. Bottom, quantification of the inhibition activity of aspirin on tube formation. *, $P < 0.05$; **, $P < 0.01$; ns, nonsignificant. **C,** The inhibitory effect of aspirin on microvessel outgrowth arising from rat aortic rings. Aortic rings were embedded in Matrigel in 96-well plates, and then fed with medium containing aspirin for 7 days. **D,** Aspirin showed anti-angiogenesis in a chorioallantoic membrane model. Glass cover-slip saturated with aspirin, suramin, or normal saline was placed at areas between preexisting vessels in the fertilized chicken eggs and incubated for 48 hours. The glass cover-slip was placed on the right side of the field.

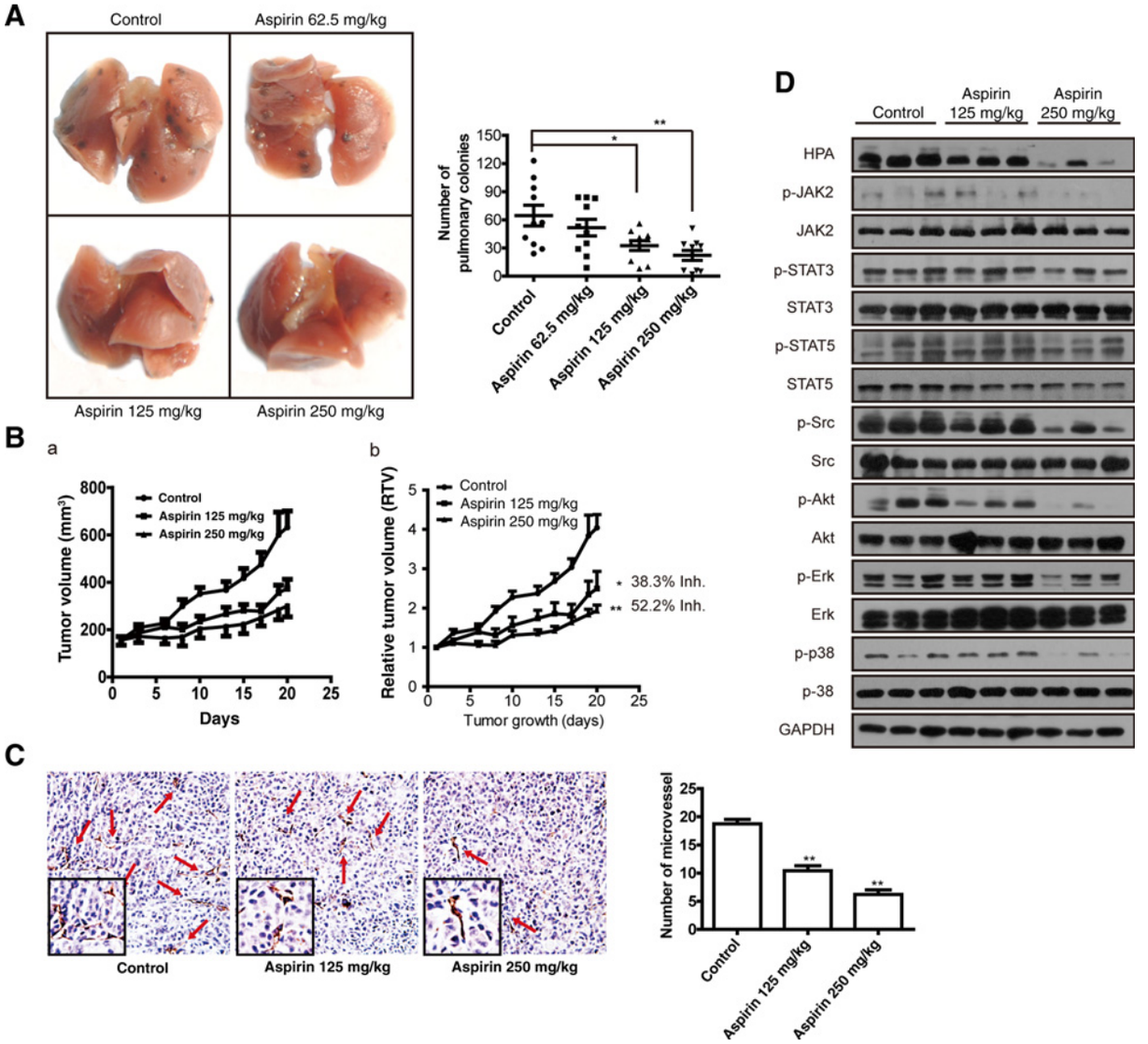

Figure 6.

Aspirin inhibits tumor metastasis, angiogenesis and growth *in vivo*. **A,** Effect of aspirin on lung metastasis of murine myeloma B16F10. Left, representative photograph of metastatic nodules on lungs. Right, The B16F10 colonies were counted and plotted. $N = 10$. **B,** Tumor growth inhibition upon aspirin treatment in MDA-MB-435 breast carcinoma xenografts. a, The curve of tumor growth after 20 days treatment of aspirin. b, Experimental inhibitory effects of aspirin on MDA-MB-435 xenografts in nude mice. The percentage of relative tumor volume (RTV) inhibition values (Inh.) was measured on the last day during the experiment. **C,** Effect of aspirin against primary tumor angiogenesis. Left, a typical photograph of immunohistochemical staining of CD31. Arrows, sites where microvessels grow. Partially enlarged views are shown in the left corner. Right, the histogram represents the number of microvessels. Similar results were obtained from at least three separate experiments. *, $P < 0.05$; **, $P < 0.01$, versus the control. **D,** Inhibition of phosphorylation of Src, STAT3, STAT5, and Erk in MDA-MB-435 xenograft by aspirin. Mice were humanely euthanized on the last day at 2 hours post-administration of aspirin and the tumors were resected. Equal amounts of proteins of tumor tissues were evaluated for phosphorylation of Src, STAT3, STAT5, and ERK levels.

observed in aspirin-treated groups, with T/C (%) of 61.7% ($P < 0.05$) and 47.8% ($P < 0.01$) at doses of 125 and 250 mg/kg, respectively (Fig. 6B). Tumor angiogenesis was assessed by measuring microvessel density using IHC analysis for CD31. At the dose of 250 mg/kg/day, the aspirin-treated groups showed a significant reduction of CD31-positive microvessels versus controls (6 ± 3 vs. 19 ± 3, respectively), with an inhibition rate of 66.9% (Fig. 6C). We also examined intratumoral heparanase level and the key downstream signaling molecules. The tumor samples were collected at 2 hours after the last administration on day 20, and we observed a marked inhibition of phospho-STAT3, phospho-Src, phospho-AKT, and phospho-Erk levels in the aspirin-treated groups (Fig. 6D).

Discussion

A growing number of studies have suggested the anticancer potential of aspirin in COX-2–independent manner (19, 22,

41–45), which are in line with increasingly recognized pharmacological activities of aspirin, including antimetastasis, antiangiogenesis, tumor microenvironment modulation, and so on. In this study, we identified heparanase as one of the potential targets of aspirin and demonstrated heparanase associated anticancer activities, particularly antimetastatic and antiangiogenic activities, which may help understand the broad activity of aspirin.

Heparanase exerted HSPG degradation triggers the release of HS chain binding angiogenic factors, such as VEGF, HGF, and bFGF, etc. (26, 27), resulting in a favorable tumor microenvironment for angiogenesis. This study showed that aspirin is able to impair VEGF release and associated angiogentic activity in a heparanase-dependent manner. Of note, previous studies have shown that aspirin and its derivatives can alter VGEF expression, leading to suppressed angiogenesis as a consequence, although how aspirin decreases VEGF expression remains unknown. These evidences together suggest that anti-angiogenic effect *in vivo* may result from collective activities of aspirin.

As an appealing target for cancer therapy, the efforts for the discovery of heparanase inhibitors have not been very successful. The current strategy for targeting heparanase is mainly concentrated on sulfuric acids or polymer anions with polysaccharide analogues. This structure allowed these compounds compete with HS binding to heparanase to inhibit the activity of heparanase. Reported heparanase inhibitors such as PI-88, PG545, and SST0001 are all close structural homologue of endogenous glycosaminoglycans (29–33). The anticoagulant agent heparin also belongs to the mimics of HS and has been used as a heparanase inhibitor. Other efforts have been expanded to heparin binding sites with KKDC, QPLK, and KKLR as proposed consensus sequences mediating the heparin/heparan sulfate–heparanase interaction. Thus far, none of the aforementioned heparanase inhibitors has made substantial progress in their anticancer property. This study identified heparanase a binding mode of aspirin that was beyond heparin-binding sites. We have shown that Lys159 and Glu225 of heparanase are critical for aspirin binding, consistent with previous findings that Glu225 and Glu343 are key residuals essential for the activity of heparanase (46, 47). Hence, we proposed a mechanism for aspirin that inhibiting the activity of heparanase by binding to Glu150 (Q9Y251: Glu 225), similar to two types of small-molecular inhibitors (48, 49). It would be interesting to further seek whether this strategy could lead to new heparanase inhibitors with improved anticancer properties.

In summary, this study has illustrated heparanase as a target of aspirin. Aspirin may directly bind to Glu150 (human Q9Y251: Glu 225) region to inhibit its enzymatic activity, thereby impeding tumor metastasis and angiogenesis both *in vitro* and *in vivo*. This study provides new insights for a better understanding of the mechanisms of aspirin in antitumor metastasis effects, and offers a new direction for the development of small-molecule inhibitors of heparanase.

Disclosure of Potential Conflicts of Interest

No potential conflicts of interest were disclosed.

Authors' Contributions

Conception and design: X. Dai, Q. Pan, D. Sun, M. Huang, X. Huang, J. Ding, M. Geng

Development of methodology: X. Dai, Q. Pan, D. Sun, X. Huang

Acquisition of data (provided animals, acquired and managed patients, provided facilities, etc.): X. Dai, J. Yan, X. Fu, Q. Pan, Y. Xu, J. Wang, L. Nie, L. Tong, A. Shen, M. Zheng, X. Huang

Analysis and interpretation of data (e.g., statistical analysis, biostatistics, computational analysis): X. Dai, Y. Xu, J. Wang, M. Zheng, M. Huang, M. Tan, X. Huang

Writing, review, and/or revision of the manuscript: X. Dai, M. Zheng, M. Huang, X. Huang, J. Ding, M. Geng

Administrative, technical, or material support (i.e., reporting or organizing data, constructing databases): X. Dai, Q. Pan, D. Sun, Y. Xu, L. Tong, A. Shen, M. Zheng, H. Liu, X. Huang

Study supervision: M. Huang, X. Huang, J. Ding, M. Geng

Grant Support

This work was supported by the "Personalized Medicines-Molecular Signature-based Drug Discovery and Development," Strategic Priority Research Program of the Chinese Academy of Sciences (No. XDA12020000, to M. Geng), NSFC-Shandong Joint Fund for Marine Science Research Centers (Grant No. U1406402, to J. Ding), Natural Science Foundation of China (No. 81302791 to X. Huang), Youth Innovation Promotion Association CAS, Shanghai Talent Development Funds (No. 201663 to X. Huang), Strategic Priority Research Program of the Chinese Academy of Sciences (No. XDA12020326 to X. Huang).

The costs of publication of this article were defrayed in part by the payment of page charges. This article must therefore be hereby marked *advertisement* in accordance with 18 U.S.C. Section 1734 solely to indicate this fact.

Received January 26, 2017; revised May 26, 2017; accepted July 10, 2017; published OnlineFirst July 14, 2017.

References

1. Thun MJ, Henley SJ, Patrono C. Nonsteroidal anti-inflammatory drugs as anticancer agents: mechanistic, pharmacologic, and clinical issues. J Natl Cancer Inst 2002;94:252–66.
2. Ruder EH, Laiyemo AO, Graubard BI, Hollenbeck AR, Schatzkin A, Cross AJ. Non-steroidal anti-inflammatory drugs and colorectal cancer risk in a large, prospective cohort. Am J Gastroenterol 2011;106:1340–50.
3. Sharpe CR, Collet JP, McNutt M, Belzile E, Boivin JF, Hanley JA. Nested case-control study of the effects of non-steroidal anti-inflammatory drugs on breast cancer risk and stage. Br J Cancer 2000;83:112–20.
4. Khuder SA, Mutgi AB. Breast cancer and NSAID use: a meta-analysis. Br J Cancer 2001;84:1188–92.
5. Cuzick J, Otto F, Baron JA, Brown PH, Burn J, Greenwald P, et al. Aspirin and non-steroidal anti-inflammatory drugs for cancer prevention: an international consensus statement. Lancet Oncol 2009;10:501–7.
6. Bosetti C, Gallus S, La Vecchia C. Aspirin and cancer risk: a summary review to 2007. Recent Res Cancer 2009;181:231–51.
7. Flossmann E, Rothwell PM, Trial BDA. Effect of aspirin on long-term risk of colorectal cancer: consistent evidence from randomised and observational studies. Lancet 2007;369:1603–13.
8. Rothwell PM, Wilson M, Elwin CE, Norrving B, Algra A, Warlow CP, et al. Long-term effect of aspirin on colorectal cancer incidence and mortality: 20-year follow-up of five randomised trials. Lancet 2010;376:1741–50.
9. Rothwell PM, Wilson M, Price JF, Belch JFF, Meade TW, Mehta Z. Effect of daily aspirin on risk of cancer metastasis: a study of incident cancers during randomised controlled trials. Lancet 2012;379:1591–601.
10. Khan MNA, Lee YS. Cyclooxygenase inhibitors: scope of their use and development in cancer chemotherapy. Med Res Rev 2011;31:161–201.
11. Qadri SSA, Wang JH, Redmond KC, O'Donnell AF, Aherne T, Redmond HP. The role of COX-2 inhibitors in lung cancer. Ann Thorac Surg 2002;74:1648–52.
12. Din FV, Valanciute A, Houde VP, Zibrova D, Green KA, Sakamoto K, et al. Aspirin inhibits mTOR signaling, activates AMP-activated protein kinase,

and induces autophagy in colorectal cancer cells. Gastroenterology 2012;142:1504–15.e3.
13. Gurpinar E, Grizzle WE, Piazza GA. NSAIDs inhibit tumorigenesis, but how? Clin Cancer Res 2014;20:1104–13.
14. Luciani MG, Campregher C, Gasche C. Aspirin blocks proliferation in colon cells by inducing a G(1) arrest and apoptosis through activation of the checkpoint kinase ATM. Carcinogenesis 2007;28:2207–17.
15. Yu HG, Huang JA, Yang YN, Huang H, Luo HS, Yu JP, et al. The effects of acetylsalicylic acid on proliferation, apoptosis, and invasion of cyclooxygenase-2 negative colon cancer cells. Eur J Clin Invest 2002;32:838–46.
16. He Y, Huang H, Farischon C, Li D, Du Z, Zhang K, et al. Combined effects of atorvastatin and aspirin on growth and apoptosis in human prostate cancer cells. Oncol Rep 2017;37:953–60.
17. Liao D, Zhong L, Duan TM, Zhang RH, Wang X, Wang G, et al. Aspirin suppresses the growth and metastasis of osteosarcoma through the NF-kappa B pathway. Clin Cancer Res 2015;21:5349–59.
18. Huang Y, Lichtenberger LM, Taylor M, Bottsford-Miller JN, Haemmerle M, Wagner MJ, et al. Antitumor and antiangiogenic effects of aspirin-PC in ovarian cancer. Mol Cancer Ther 2016;15:2894–904.
19. Lu M, Strohecker A, Chen F, Kwan T, Bosman J, Jordan VC, et al. Aspirin sensitizes cancer cells to TRAIL-induced apoptosis by reducing survivin levels. Clin Cancer Res 2008;14:3168–76.
20. Domingo E, Church DN, Sieber O, Ramamoorthy R, Yanagisawa Y, Johnstone E, et al. Evaluation of PIK3CA mutation as a predictor of benefit from nonsteroidal anti-inflammatory drug therapy in colorectal cancer. J Clin Oncol 2013;31:4297–305.
21. Reimers MS, Bastiaannet E, Langley RE, van Eijk R, van Vlierberghe RLP, Lemmens VEP, et al. Expression of HLA class I antigen, aspirin use, and survival after a diagnosis of colon cancer. JAMA Intern Med 2014; 174:732–9.
22. Zumwalt TJ, Wodarz D, Komarova NL, Toden S, Turner J, Cardenas J, et al. Aspirin-induced chemoprevention and response kinetics are enhanced by PIK3CA mutations in colorectal cancer cells. Cancer Prev Res 2017;10:208–18.
23. Li JP, Vlodavsky I. Heparin, heparan sulfate and heparanase in inflammatory reactions. Thromb Haemost 2009;102:823–8.
24. Vlodavsky I, Elkin M, Pappo O, Aingorn H, Atzmon R, Ishai-Michaeli R, et al. Mammalian heparanase as mediator of tumor metastasis and angiogenesis. Isr Med Assoc J 2000;2Suppl:37–45.
25. Pikas DS, Li JP, Vlodavsky I, Lindahl U. Substrate specificity of heparanases from human hepatoma and platelets. J Biol Chem 1998;273:18770–7.
26. Talmadge JE, Fidler IJ. AACR centennial series: the biology of cancer metastasis: historical perspective. Cancer Res 2010;70:5649–69.
27. Vlodavsky I, Friedmann Y. Molecular properties and involvement of heparanase in cancer metastasis and angiogenesis. J Clin Invest 2001; 108:341–7.
28. Dong W, Zhao H, Zhang C, Geng P, Sarengaowa, Li Q, et al. Gene silencing of heparanase results in suppression of invasion and migration of hepatoma cells. World J Surg Oncol 2014;12:85.
29. McKenzie EA. Heparanase: a target for drug discovery in cancer and inflammation. Br J Pharmacol 2007;151:1–14.
30. Liu CJ, Chang J, Lee PH, Lin DY, Wu CC, Jeng LB, et al. Adjuvant heparanase inhibitor PI-88 therapy for hepatocellular carcinoma recurrence. World J Gastroenterol 2014;20:11384–93.
31. Liang XJ, Yuan L, Hu J, Yu HH, Li T, Lin SF, et al. Phosphomannopentaose sulfate (PI-88) suppresses angiogenesis by downregulating heparanase and vascular endothelial growth factor in an oxygen-induced retinal neovascularization animal model. Mol Vis 2012;18:1649–57.
32. Ostapoff KT, Awasthi N, Cenik BK, Hinz S, Dredge K, Schwarz RE, et al. PG545, an angiogenesis and heparanase inhibitor, reduces primary tumor growth and metastasis in experimental pancreatic cancer. Mol Cancer Ther 2013;12:1190–201.
33. Cassinelli G, Lanzi C, Tortoreto M, Cominetti D, Petrangolini G, Favini E, et al. Antitumor efficacy of the heparanase inhibitor SST0001 alone and in combination with antiangiogenic agents in the treatment of human pediatric sarcoma models. Biochem Pharmacol 2013;85:1424–32.
34. Altschul SF, Gish W, Miller W, Myers EW, Lipman DJ. Basic local alignment search tool. J Mol Biol 1990;215:403–10.
35. Michikawa M, Ichinose H, Momma M, Biely P, Jongkees S, Yoshida M, et al. Structural and biochemical characterization of glycoside hydrolase family 79 beta-glucuronidase from Acidobacterium capsulatum. J Biol Chem 2012;287:14069–77.
36. Sali A, Blundell TL. Comparative protein modelling by satisfaction of spatial restraints. J Mol Biol 1993;234:779–815.
37. Zhao H, Liu H, Chen Y, Xin X, Li J, Hou Y, et al. Oligomannurarate sulfate, a novel heparanase inhibitor simultaneously targeting basic fibroblast growth factor, combats tumor angiogenesis and metastasis. Cancer Res 2006;66:8779–87.
38. Chen Y, Kwon SW, Kim SC, Zhao Y. Integrated approach for manual evaluation of peptides identified by searching protein sequence databases with tandem mass spectra. J Proteome Res 2005;4:998–1005.
39. Li MY, Lv YC, Tong LJ, Peng T, Qu R, Zhang T, et al. DW10075, a novel selective and small-molecule inhibitor of VEGFR, exhibits antitumor activities both in vitro and in vivo. Acta Pharmacol Sin 2016;37:398–407.
40. Sapay N, Cabannes E, Petitou M, Imberty A. Molecular model of human heparanase with proposed binding mode of a heparan sulfate oligosaccharide and catalytic amino acids. Biopolymers 2012;97:21–34.
41. Yan F, He QZ, Hu X, Li W, Wei K, Li L, et al. Direct regulation of caspase-3 by the transcription factor AP-2 alpha is involved in aspirin-induced apoptosis in MDA-MB-453 breast cancer cells. Mol Med Rep 2013; 7:909–14.
42. Alfonso LF, Srivenugopal KS, Arumugam TV, Abbruscato TJ, Weidanz JA, Bhat GJ. Aspirin inhibits camptothecin-induced p21CIP1 levels and potentiates apoptosis in human breast cancer cells. Int J Oncol 2009; 34:597–608.
43. Marimuthu S, Chivukula RSV, Alfonso LF, Moridani M, Hagen FK, Bhat GJ. Aspirin acetylates multiple cellular proteins in HCT-116 colon cancer cells: identification of novel targets. Int J Oncol 2011;39:1273–83.
44. Henry WS, Laszewski T, Tsang T, Beca F, Beck AH, McAllister SS, et al. Aspirin suppresses growth in PI3K-mutant breast cancer by activating AMPK and inhibiting mTORC1 signaling. Cancer Res 2017;77:790–801.
45. Roh JL, Kim EH, Jang H, Shin D. Aspirin plus sorafenib potentiates cisplatin cytotoxicity in resistant head and neck cancer cells through xCT inhibition. Free Radical Bio Med 2017;104:1–9.
46. Hulett MD, Hornby JR, Ohms SJ, Zuegg J, Freeman C, Gready JE, et al. Identification of active-site residues of the pro-metastatic endoglycosidase heparanase. Biochemistry 2000;39:15659–67.
47. Goldshmidt O, Zcharia E, Cohen M, Aingorn H, Cohen I, Nadav L, et al. Heparanase mediates cell adhesion independent of its enzymatic activity. FASEB J 2003;17:1015–25.
48. Ishida K, Hirai G, Murakami K, Teruya T, Simizu S, Sodeoka M, et al. Structure-based design of a selective heparanase inhibitor as an antimetastatic agent. Mol Cancer Ther 2004;3:1069–77.
49. Vinader V, Haji-Abdullahi MH, Patterson LH, Afarinkia K. Synthesis of a pseudo-disaccharide library and its application to the characterisation of the heparanase catalytic site. PLoS One 2013;8:e82111.